ChemComm

Accepted Manuscript

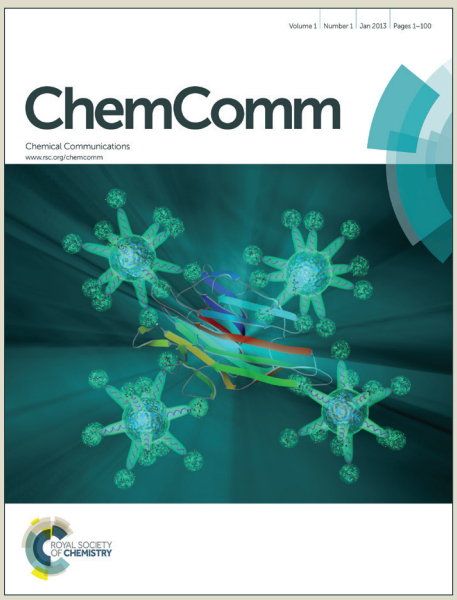

ROYAL SOCIETY OF CHEMISTRY

www.rsc.org/chemcomm

Cite this: DOI: 10.1039/coxx00000x

www.rsc.org/xxxxxx

ARTICLE TYPE

Enhanced Quantum Yield of Nitrogen Fixation for Hydrogen Storage with In-Situ-Formed Carbonaceous Radicals

Weirong Zhao* , Haiping Xi, Meng Zhang, Yajun Li, Jinsheng Chen, Jing Zhang, and Xi Zhu

Received (in XXX, XXX) Xth XXXXXXXXX 20XX, Accepted Xth XXXXXXXXX 20XX

DOI: 10.1039/b000000x

NH_3 is a potential hydrogen energy carrier. Here we use alcohols as hole scavengers to investigate the nitrogen photofixation mechnisms including direct and indirect electron transfer processes. The *t*-butanol system exhibited the highest quantum yield of 36.1%, ascribing to the in-situ-formed indirect electronic transmitter of $\bullet CO_2^-$.

Hydrogen, as a green energy source with a very high gravimetric energy content (120 MJ kg^{-1}),[1] has received extensive attention.[2] According to Klerke,[3] when 10 kg of hydrogen (14 g L^{-1}, 200 bar) is stored, the hydrogen density is 71 g L^{-1} in its liquid phase (−252 °C) and up to 108 g L^{-1} in the form of liquid NH_3 (one of the storage forms of hydrogen). NH_3 is produced on a large scale and can be easily liquefied at room temperature (ca. 10 bar).[1] Moreover, liquid NH_3 is much easier to obtain and safer to handle compared to liquid hydrogen. Given that the hydrogen storage capacity of 1 mol of NH_3 is 1.5 mol of H_2 (based on 1 mol of hydrogen production), compared to water splitting[4] ($H_2O \rightarrow H_2(g) + 1/2O_2(g)$, $\Delta H = 285$ kJ mol^{-1}), the total energy demand via NH_3 synthesis ($1/2N_2(g) + 3/2H_2O(g) \rightarrow NH_3(g) + 3/4O_2(g)$, $\Delta H = 317$ kJ mol^{-1})[5] and decomposition ($NH_3(g) \rightarrow 3/2H_2(g) + 1/2N_2(g)$, $\Delta H = 46.0$ kJmol^{-1})[3] is lower (approximately 242 kJ mol^{-1}). In addition, NH_3 is the only carbon-free carrier solution of hydrogen;[6] thus, it can be used in fuel cell systems without releasing CO_x. With its advantages of high energy density, convenient storage, thermodynamical properties and environment-friendly features, NH_3 is a promising alternative energy carrier.[3,6] Industrial methods for NH_3 synthesis have been well studied and developed. Typically, NH_3 is synthesized under harsh conditions (300−550 °C, 150−250 atm) using an iron catalyst;[7] in addition, this method consumes a large amount of energy. Thus, the development of NH_3 generation systems that operate under mild conditions is of interest. Photofixation with suitable semiconductor photocatalysts under ambient conditions has been considered.[8] Rusina *et al.* extensively studied nitrogen photofixation ($\lambda \geq$ 320 nm) on iron titanate films;[8c, 9] however, the yield was far from satisfactory. In the presence of 75 vol% ethanol, the concentration of NH_3 generated was only 1.7×10^{-5} mol L^{-1}. We have previously used Fe-doped TiO_2 as a photocatalyst, resulting in the highest reported generation amount of 1.2×10^{-3} mol L^{-1} in the presence of 1.7×10^{-2} mol L^{-1} ethanol as a hole scavenger.[10] Hole scavengers play an important role in significantly enhancing the NH_3 yield.

Herein, we chose biomass platform products (*e.g.* alcohols) as scavengers to investigate their effects on photocatalytic nitrogen fixation under UV irradiation (λ = 254 nm) using uniform and stable mesoporous β-Ga_2O_3 nanorods as a photocatalyst (ESI, Experimental details†). β-Ga_2O_3, with a 4.4 eV wide bandgap, effectively inhibits the recombination of intrinsic optical carriers and exhibits strong photocatalytic ability. The activity of β-Ga_2O_3 is further promoted by the use of alcohols as hole scavengers. Using methanol, ethanol, *n*-propanol, and *n*-butanol as hole scavengers, the turnover efficiencies (TOF) were 2.95×10^{-6}, 1.02×10^{-6}, 7.52×10^{-7}, and 4.93×10^{-7} mol g^{-1} s^{-1}, respectively (ESI, Table S1†), whereas the quantum yields of the photocatalytic hydrogen storage were 12.5%, 4.35%, 3.19%, and 2.10%, respectively (Fig. 1 and ESI, Table S1†). In the case of β-Ga_2O_3, which is an *n*-type semiconductor, E_{CB} is negatively shifted approximately 0.1 V from the flat-band potential (V_{fb})[11] derived from the Mott-Schottky plot (ESI, Fig. S1†) and equation[8a, 10, 11b] (ESI, Eq. S2†). Thus, the E_{CB} of β-Ga_2O_3 is approximately −0.53 V. When β-Ga_2O_3 is subjected to UV irradiation, photo-generated holes (E_{VB} = 3.87 V) can oxidize OH^- to •OH ($E_{\bullet OH/OH^-}$ = 1.985 V vs. SHE),[10] which can be captured by alcohols. Thus, the light-generated electrons on the surface of β-Ga_2O_3 can directly reduce N_2 to NH_3 ($E_{N2/NH3}$ = −0.092 V vs. SHE):[10]

$$N_2 + 6H^+ + 6e^- \rightarrow 2NH_3 \quad (1)$$

Alcohols with lower E_{HOMO} (energy of the highest occupied

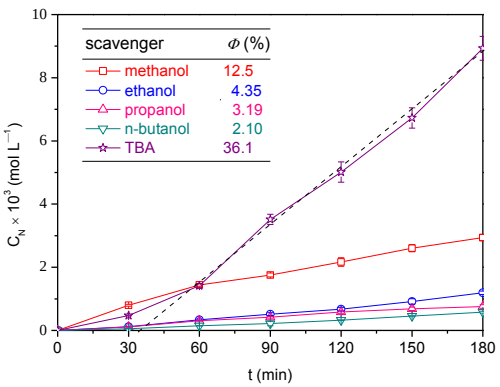

Fig 1 Nitrogen photofixation of β-Ga_2O_3 in 100 mL of solution containing 0.02 mol L^{-1} alcohol hole scavengers under irradiation of 254 nm at pH 7 and 25 ℃. Φ: quantum yield; C_N: concentration of NH_3-N.

molecular orbital) can be more easily oxidized. Using Gaussian calculations,[12] we determined that the E_{HOMO} values of methanol, ethanol, *n*-propanol, and *n*-butanol were −13.776, −13.700, −13.698, and −13.696 eV, respectively (ESI, Table S1†). Among the investigated alcohols, methanol can lose electrons most easily, whereas ethanol, *n*-propanol, and *n*-butanol exhibit moderate abilities to lose electrons, thereby indicating that electron donating ability may decrease with increasing carbon number of the alcohols. When *t*-butanol (TBA) was used as a hole scavenger, the obtained quantum yield (Fig. 1 and ESI, Table S1†) was 36.1%, which is nearly 3 times that obtained with methanol. It is almost 2 times that best obtained in our previously reported work with ethanol as hole scavenger and Fe-TiO_2 (atomic ratio of Fe and Ti is 1) as photocatalyst. Given that the E_{HOMO} of TBA is −13.311 V, which is more positive than the E_{HOMO} values of the other alcohols, we attributed this high quantum yield to the indirect electron transfer rate caused by high yield of in-situ-formed $\bullet CO_2^-$ in TBA systems. As shown in the TBA reaction curve, the slope increases significantly after 35 min, suggesting that the reaction consists of two stages in which the reaction rate is notably increased in the second stage. When the TBA concentration was increased from 0.005 to 0.1 mol L^{-1}, the quantum yield of N_2 fixation increased from 20.8% to 38.8% (ESI, Fig. S2†) and the onset of the second stage shifted from 75 min to 25 min. This result is reasonably speculated to have occurred as a result of the increased formation rate of $\bullet CO_2^-$. When the TBA concentration was less than 0.01 mol L^{-1}, the reaction rate decreased after 150 min because the depletion of TBA decreased the formation of $\bullet CO_2^-$, thus slowing the indirect electron transfer rate.

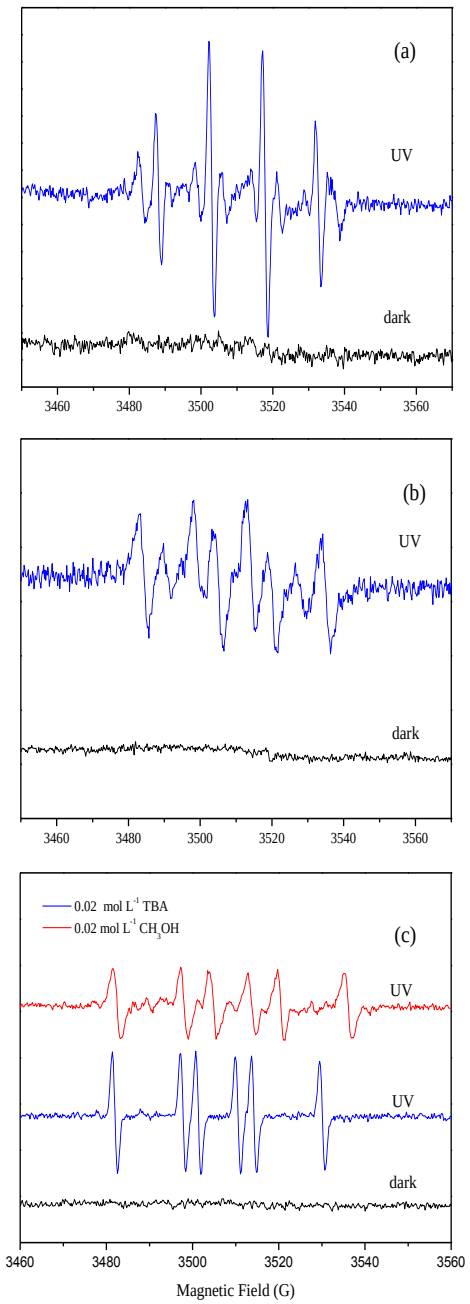

Fig.2 ESR spectra of β-Ga_2O_3 in dark and under UV irradiation of 254 nm. (a) DMPO–•OH in water, (b) DMPO–$\bullet O_2^-$ in methanol, and (c) DMPO–$\bullet CO_2^-$ in 0.2 mol L^{-1} TBA and CH_3OH.

The presence of $\bullet CO_2^-$ was confirmed by electron spin resonance (ESR) (Fig. 2). No ESR signals were observed when samples were measured in the dark. Under UV irradiation, a suspension of β-Ga_2O_3 yielded the well-characterized DMPO-OH• and •DMPO-O_2^- adducts (Fig. 2a and b). When CH_3OH was added to the system, characteristic peaks nearly identical to those of the previously reported •DMPO-CO_2^- were observed[13] (Fig. 2c). When TBA was added to the system, no •OH was detected in the ESR spectrum (Fig. 2c), and the characteristic peak intensity of $\bullet CO_2^-$ was stronger than that of CH_3OH. The high peak intensity of $\bullet CO_2^-$ is ascribed to the increased formation rate of $\bullet CO_2^-$, which leads to the enhancement of the indirect electron transfer rate. The strong reducing ability of $\bullet CO_2^-$ ($E_{CO2/\bullet CO2-}$ = −1.9 to −1.8 V)[13-14] can facilitate the reduction of N_2 to NH_3 (Eq. 2), which, in turn, accounts for the high quantum yield in the TBA system.

$$N_2 + 6\bullet CO_2^- + 2H_2O \rightarrow 2NH_3 + 6OH^- + 6CO_2 \quad (2)$$

Fig. 3 further shows the role of indirect electron transfer caused by $\bullet CO_2^-$ under a different reaction atmosphere. In a 4:1 N_2/Ar system, most photo-generated electrons flowed directly to N_2; thus, the reaction is generally regarded as a direct electron transfer process. The N_2/O_2 (4:1) system achieved the higher quantum yield, up to 36.0%, which was 2.15 times greater than that of the N_2/Ar (4:1) system. These results are attributed to the role of oxygen, which can be reduced to $\bullet O_2^-$ ($E_{O2/\bullet O2-}$ = −0.284 V vs. SHE)[10] by electrons (E_{CB} = −0.53 V). The generated $\bullet O_2^-$ converts into •OH[15] and quickly reacts with TBA to finally form $\bullet CO_2^-$. Figure S5 shows the concentration changes of H_2O_2 during the reaction process, as measured using UV spectrophotometry. The amount of H_2O_2 produced was lowest for the TBA systems—almost 25% less than the amounts produced by the other systems. This finding may be related to the excellent •OH scavenging ability of TBA and to most of the H_2O_2 produced in the TBA system converting into •OH and being quickly consumed during the reaction.[14a] Thus, we hypothesize

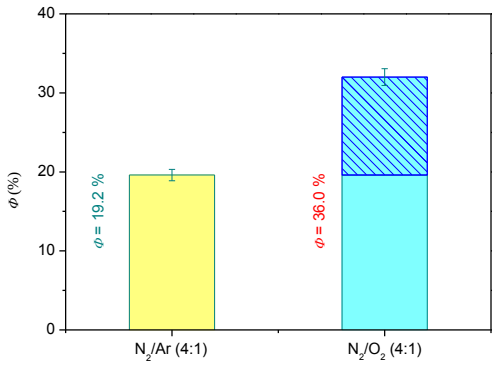

Fig. 3 Nitrogen photofixation efficiency of β-Ga_2O_3 with 0.02 mol L^{-1} TBA as a hole scavenger under different atmospheres.

that the other indirect reaction pathways are as follows:

$O_2 + e^- \rightarrow \bullet O_2^-$ (3)

$2\bullet O_2^- + 4H_2O \rightarrow 3H_2O_2 + 2OH^-$ (4)

$H_2O_2 + e^- \rightarrow \bullet OH + OH^-$ (5)

$OH^- + h^+ \rightarrow \bullet OH$ (6)

$\bullet OH + TBA \rightarrow \bullet CO_2^- + intermediates$ (7)

The N_2/O_2 (4:1) system was composed of direct and indirect electron transfer processes, in which the direct electron transfer accounted for 46.7% of the total amount of photocatalytic hydrogen storage and the indirect nitrogen fixation accounted for 53.3%.

Fig. S3 (ESI†) displays the distribution of intermediates during the hydrogen storage process via quadrupole time-of-flight mass spectrometry (Q-TOF-MS) of the TBA systems. Peaks corresponding to $[N_2H_4+H]^+$ (33.0526 amu) and $[TBA+H]^+$ (75.1243 amu) are clearly shown. When a xylene/aminobenzaldehyde UV spectrophotometry method was employed using a detection wavelength of 458 nm, N_2H_4 was also detected at a concentration of 1.30×10^{-6} mol L^{-1}. The generated N_2H_4 or NH_3 was therefore reasonably presumed to react with carbonaceous intermediates to form isomers of C_6H_9NO (111.0246 amu) or other nitrogen-containing by-products. A small amount of carbonaceous matter, such as $C_8H_{10}O_2$ (138.0461 amu), was also detected; the matter may consist of dimers resulting from reactions between TBA and various free radicals. On the basis of the intermediate and final products, density functional theory (DFT) calculations were used to investigate the transition state and the intrinsic electron transfer pathways during the hydrogen storage process (ESI, Fig. S4 and Table S2†). According to Hoffman *et al.*,[16] the possible intermediate states are $\bullet N_2$=N-, HN=N-, •HN-NH-, H_2N-NH-, H_2N-NH_2, and $\bullet NH_2$, similar to our previous results.[10] According to our previous report[10], the reaction in nitrogen photofixation system mainly occurs on the catalyst surface, and the active H• derived from H_2O on the surface of catalyst plays an important role, which is in accordance with rusina *et al.*'s research. As shown in Table S2† (ESI), the N-Ga distances range between 1.961 and 2.667 Å, and the adsorption energies are all negative, indicating that these intermediates can be relatively stably adsorbed onto the catalyst surface. Therefore, these results suggest that the dominant nitrogen fixation steps occur on the surface of β-Ga_2O_3 and that the electron transfer is caused directly by photo-generated carriers or indirectly by in-situ-formed carbonaceous radicals. Because the N-Ga distances of H_2N−NH_2 and NH_3 are slightly larger than that of several other intermediate states, they should tend to desorb from the surface of β-Ga_2O_3. This hypothesis was verified by the detection of N_2H_4 and NH_3 in the suspension. In the transformation process from N≡N···Ga to H_2N−NH_2···Ga, the N-N bond length increases gradually from 1.159 to 1.464 Å and tends toward N−N separation, which is also confirmed by the generation of NH_3. Fig. 4 clearly shows the aforementioned intermediate conversion process during direct (1) and indirect (2) electron transfer pathways.

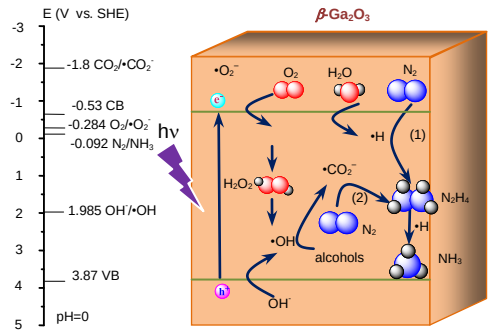

Fig. 4 Speculated direct (1) and indirect (2) electron transfer pathways

Conclusions

In summary, a high quantum yield of nitrogen fixation, as high as 36.1%, was achieved via the combined action of indirect electron transfer induced by in-situ-formed $\bullet CO_2^-$ and direct electron transfer on the surface of photocatalysts. Furthermore, O_2 improved the efficiency of photocatalytic hydrogen storage instead of suppressing the conversion of N_2 into NH_3. This finding has important implications for future research related to nitrogen fixation for hydrogen storage systems. In our work, all the biomass-derivated alcohols, as scavengers, had more or less promoted the nitrogen fixation process. Other easily accessible biomass (*e.g.* glucide, aldehydesacids, and esters) will be our ongoing researching scavengers, which will give some hints about obtaining new green energy using electrons provided by pollutants during degradation.

Acknowledgements

The work is supported by the National Natural Science Foundation of China (Grants 51178412 and 51278456) and the National Key Technologies R&D Program of China (Grant 2013BAC16B01).

Notes and references

Department of Environmental Engineering, Zhejiang University, 866 Yu Hang Tang Road, Hangzhou 310058, China. Fax: +86 571 8898 2032; Tel: 86 571 8898 2032; E-mail: weirong@mail.hz.zj.cn

† Electronic Supplementary Information (ESI) available: Experimental details; Fig.S1-S4, time courses for NH_3 generation with different TBA concentrations, Q-TOF-MS spectra, time courses for H_2O_2 generation, DFT calculation structures; Table S1-S2, some parameters and DFT calculation results . See DOI: 10.1039/b000000x/

1 W. I. David, J. W. Makepeace, S. K. Callear, H. M. Hunter, J. D. Taylor, T. J. Wood and M. O. Jones, *J. Am.Chem. Soc.*, 2014. **136**, 13082.

2 (a) M. Ball and M. Wietschel, *Int. J. Hydrogen Energy*., 2009, **34**, 615; (b) G. Deluga, J. Salge, L. Schmidt and X. Verykios, *Science.*, 2004, **303**, 993; (c) Q. Li, B. Guo, J. Yu, J. Ran, B. Zhang, H. Yan and J. R. Gong, *J. Am. Chem. Soc.*, 2011, **133**, 10878; (d) R. Navarro, M. Sanchez-Sanchez, M. Alvarez-Galvan, F. Del Valle and J. Fierro, *Energy Environ. Sci.*, 2009, **2**, 35; (e) D. Zhao, D. Yuan and H. Zhou, *Energy Environ. Sci.*, 2008, **1**, 222.

3 A. Klerke, C. H. Christensen, J. K. Nørskov and T. Vegge, *J. Mater. Chem.*, 2008, **18**, 2304.

4 C. Rozain and P. Millet, *Electrochim. Acta*., 2014, **131**, 160.

5 R. Perkins, B. Mattson, J. Fujita, R. Catahan, W. Cheng, J. Greimann, T. Hoette, P. Khandhar, A. Mattson and A. Rajani, *J. Chem. Educ.*, 2003, **80**, 768.

6 F. Schüth, R. Palkovits, R. Schlögl and D. Su, *Energy Environ. Sci.*, 2012, **5**, 6278.

7 D. Zhu, L. Zhang, R. E. Ruther and R. J. Hamers, *Nat. Mater.*, 2013, **12**, 836.

8 (a) K. Hoshino, R. Kuchii and T. Ogawa, *Appl. Catal., B*, 2008, **79**, 81; (b) O. Linnik and H. Kisch, *Photochem. Photobiol. Sci*., 2006, **5**, 938; (c) O. Rusina, A. Eremenko, G. Frank, H. P. Strunk and H. Kisch, *Angew. Chem., Int. Ed.*, 2001, **40**, 3993.

9 (a) O. Rusina, O. Linnik, A. Eremenko and H. Kisch, *Chem. - Eur. J.*, 2003, **9**, 561; (b) O. Rusina, W. Macyk and H. Kisch, *J. Phys. Chem. B.*, 2005, **109**, 10858.

10 W. Zhao, J. Zhang, X. Zhu, M. Zhang, J. Tang, M. Tan and Y. Wang, *Appl. Catal., B.*, 2014, **144**, 468.

11 (a) H. Huang, D. Li, Q. Lin, Y. Shao, W. Chen, Y. Hu, Y. Chen and X. Fu, *J. Phys. Chem. C.*, 2009, **113**, 14264; (b) J. Lv, T. Kako, Z. Li, Z. Zou and J. Ye, *J. Phys. Chem. C.*, 2010, **114**, 6157.

12 G. Gece and S. Bilgiç, *Corros. Sci.*, 2010, **52**, 3435.

13 L. L. Perissinotti, M. A. Brusa and M. A. Grela, *Langmuir.*, 2001, **17**, 8422.

14 (a) N. M. Dimitrijevic, B. K. Vijayan, O. G. Poluektov, T. Rajh, K. A. Gray, H. He and P. Zapol, *J. Am.Chem. Soc.*, 2011, **133**, 3964; (b) J. Lee, W. Choi and J. Yoon, *Environ. Sci. Technol.*, 2005, **39**, 6800.

15 K. Nagaveni, M. Hegde, N. Ravishankar, G. Subbanna and G. Madras, *Langmuir.*, 2004, **20**, 2900.

16 B. M. Hoffman, D. R. Dean and L. C. Seefeldt, *Acc. Chem. Res.*, 2009, **42**, 609.